CIRP Annals - Manufacturing Technology 60 (2011) 137–140

Contents lists available at ScienceDirect

CIRP Annals - Manufacturing Technology

journal homepage: http://ees.elsevier.com/cirp/default.asp

Control of deformation levels on machined surfaces

Y. Guo [a], R. M'Saoubi (2)[b,*], S. Chandrasekar [a]

[a] Center for Materials Processing and Tribology, School of Industrial Engineering, Purdue University, West Lafayette, IN, USA
[b] R&D Materials and Technology Development, Seco Tools AB, Fagersta, Sweden

ARTICLE INFO

Keywords:
Machining
Surface
Deformation
Microstructure

ABSTRACT

Deformation history of machined surface in low-speed cutting has been characterized using image correlation, complemented by hardness and microstructure analyses. Scaling of subsurface strain distribution, and large surface strains are observed. Similarity in deformation history of chip and near-surface suggests a framework for engineering surfaces with controlled deformation levels and microstructures, directly, by machining. The deformation characterization offers scope also for improvement of machining models.

A principal objective of machining is creation of component surfaces with specific attributes that enable functionality of products. From a surface integrity standpoint, deformation levels and microstructure are perhaps the most critical, since these determine mechanical and physical properties [1,2]. While microstructure engineering by deformation control underpins the majority of research in deformation processing [3], these aspects have received less attention in machining. Control of attributes has been focused almost exclusively on achieving desired topography, and to a lesser extent residual stress, the latter due to its influence on fatigue life [4–6]. In contrast, residual plastic strains, which are likely to impact fatigue properties and wear, have been the subject of few investigations. Recent research in Severe Plastic Deformation (SPD) has demonstrated, at least in a conceptual way, the complex interrelationship between deformation and microstructure evolution [7,8]. Since surface generation occurs by imposition of extreme strains into millimeter sized domains, these developments in SPD suggest opportunities for engineering surfaces with graded microstructures and novel properties, directly, by machining. Central to these opportunities is an understanding of the deformation history of the machined surface, the focus of the present study.

1. Background

To understand the deformation history on a machined surface, it is useful to examine surface generation by chip formation. Chip formation occurs by SPD in a narrow zone – primary deformation zone – ahead of the tool cutting edge, see Fig. 1. Large plastic strains (1–15) are imposed in the chip, the strains depending on the rake angle and deformation geometry. Bulk and particulate ultrafine grained (UFG) alloys have been successfully produced by chip formation (SPD) [8,9]. Since the primary deformation zone permeates the subsurface of the workpiece [9,10], the deformation and microstructure on the surface are also determined by the time history of the SPD that the material constituting the surface experiences. This deformation will be enhanced by rubbing occurring in the vicinity of the cutting edge, the enhancement being determined by the local geometry of the edge. Further modulation of the deformation due to temperature may be expected at high cutting speeds leading to phenomena such as recrystallization and phase transformations. The occurrence of large strains on machined surfaces is supported by microstructure observations. Copper surfaces created by polishing or 'grinding' with a rotating spherical tool consist of UFG microstructures with ~100 nm grain size [11,12]. The widely studied 'white etching layer' is a notable example of a UFG surface layer that has its origins, at least partially in SPD. Electron Backscatter Diffraction (EBSD) analysis of machined stainless steel and Ni-based alloys indicates that the subsurface microstructure is also UFG [13]. While occurrence of UFG microstructures on surfaces has been recognized, engineering of these structures by controlling SPD parameters (e.g., strain, strain rate) appears to have received little consideration. Recent studies of deformation in machining suggest this possibility [8,9], which is advanced in the present study.

2. Experimental

Plane strain machining experiments were carried out using a sharp high speed steel tool to cut 70 Cu–30 Zn brass (grain size 200 μm, 80 HV) and commercially pure (99.99%) OFHC copper (grain size 35 μm, 77 HV); this included experiments with Cu at ~ −196 °C by immersing the workpiece in liquid nitrogen (cryo-machining). The objective was to study evolution of deformation on the surface in terms of strain and strain rate, and hardness and microstructure. The choice of work material was influenced by prior studies of SPD. Shear strains of 1–10 were imposed by varying the rake angle, and the cutting speed (v_c) was varied between 1 and 50 mm/s. The small values of speed minimized temperature influences. A linear machining arrangement was employed, with the workpiece (50 mm length × 25 mm height × 2 mm width) being moved with respect to the tool using a DC motor. Cutting was done on the 50 mm × 2 mm side with the tool held stationary on a

* Corresponding author.

0007-8506/$ – see front matter © 2011 CIRP.
doi:10.1016/j.cirp.2011.03.138

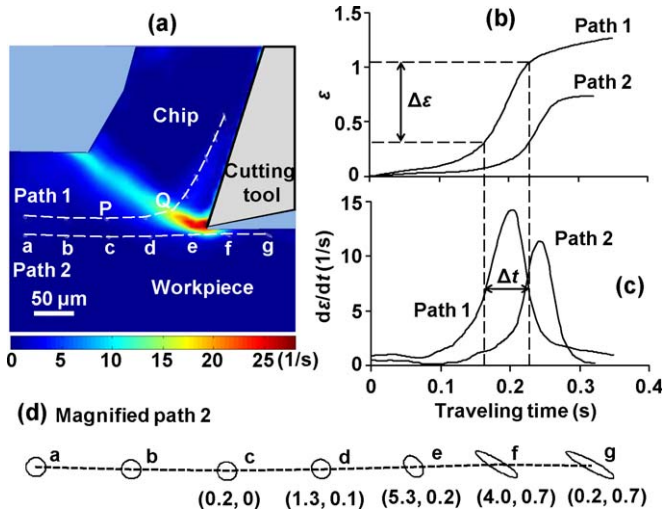

Fig. 1. Deformation in machining of brass showing (a) effective strain rate field; variation of (b) strain and (c) strain rate along paths 1 and 2; and (d) deformation history of a circle element along path 2 which becomes part of workpiece. The coordinates represent ($d\varepsilon/dt$, ε) at various points along path 2. $\gamma = +20°$, $h_o = 100$ μm, and $v_c = 1$ mm/s.

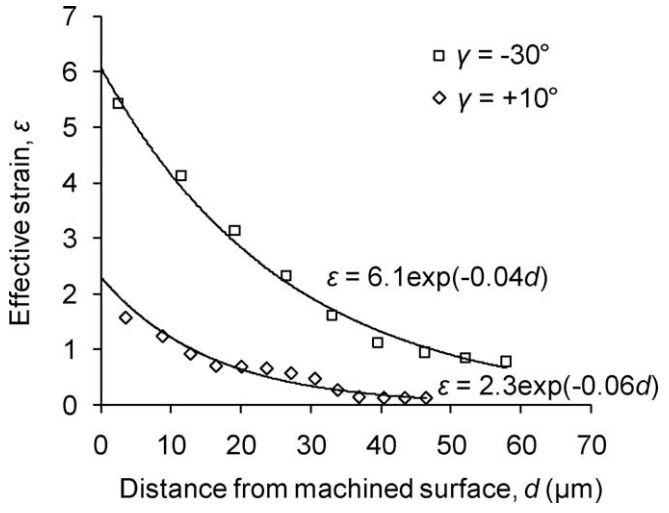

Fig. 2. Variation of strain with distance (d) from machined surface. Brass, $h_o = 150$ μm, $v_c = 10$ mm/s.

holder fixed to a vertical stage. The rake angle (γ) was adjusted by changing the orientation of the tool holder and the undeformed chip thickness (h_o) by moving the stage [8]. A sharp cutting edge, to minimize rubbing-deformation, was ensured by grinding of clearance and rake faces without additional polishing.

Deformation parameters were measured using Particle Image Velocimetry (PIV), an image analysis technique [14]. One side of the machining zone (typically 500 × 500 μm) was imaged at up to 2000 frames per second and a spatial resolution of ~0.4 μm per pixel, using a high-speed CMOS camera coupled to a microscope assembly. The images were analyzed using PIV to estimate displacement/velocity fields in the deformation zone and workpiece. Strain rate/strain tensors and effective values were derived from the displacement field [8,14]. Chip strain was estimated also by the shear plane model utilizing PIV-based velocities. Hardness on chip and machined surface was measured using nano- and Vickers-indentation, complemented by microstructure analyses with EBSD and Transmission Electron Microscopy (TEM).

3. Results

3.1. Deformation levels on machined surface

Fig. 1a shows a typical effective (von Mises) strain rate field in machining brass obtained using PIV. The region of large strain rate is the primary deformation zone. This correspondence is important since the zone is often confused with a region of large strain. The deformation zone is seen to be narrow (~20 μm thick) and relatively uniform (strain rate ~10/s), except for a small pocket of larger strain rate (~25/s) near the cutting edge. Fig. 1b and c shows effective strain (ε) and strain rate ($d\varepsilon/dt$) values as a function of time – deformation histories – along 2 paths, path 1 entering the chip and path 2 becoming part of the work surface. The strain increases quite rapidly as a particle crosses the deformation zone and then becomes constant, indicating that the deformation has ceased (Fig. 1b); this constant value is the total strain imposed. The strain rate experienced by a particle exhibits a peak inside the deformation zone (Fig. 1c). A representative value may be assigned for this rate as $d\varepsilon/dt = \Delta\varepsilon/\Delta t$, where Δt is the half-width of the peak (Fig. 1c), and $\Delta\varepsilon$ is the corresponding strain increment (Fig. 1b). For the example shown, this value is ~12/s. Due to deformation, a circle element in the initial workpiece transforms into an ellipse, see path 2 in Fig. 1d, with coordinates at the various points representing (strain rate, strain). The strain rate tensor can be estimated at various points. For example, at P and Q, it is given by $\begin{bmatrix} -1.0 & -1.1 \\ -1.1 & 0.6 \end{bmatrix}$ and $\begin{bmatrix} -7.3 & -5.3 \\ -5.3 & 9.5 \end{bmatrix}$ (1/s), respectively, where P is located near the entrance of the deformation zone and Q is within the strain-rate peak inside the zone. The (+ve) x-axis is parallel to v_c and to the right, while the (+ve) y-axis is taken to point up (Fig. 1). The time histories of strain rate tensors determine crystallographic texture evolution.

Using various particle paths, deformation histories and residual plastic strains were obtained for the workpiece and chip. Deformation levels on the surface were obtained by extrapolating near-surface measurements. Fig. 2 shows the variation of strain with distance (d) from surface in brass for $\gamma = -30°$ and $+10°$. The strain decreases rapidly with distance from the surface. When the strain data are fitted with exponential functions, based on analogy with sliding [1], the function intercepts with the vertical axis give the residual surface strains as 6.1 and 2.3, respectively, for $\gamma = -30°$ and $+10°$, confirming SPD on the surface. The increase in surface strain with decreasing rake angle is similar to that for chip strain, suggesting the possibility of controlling surface strain using γ. If the deformed zone is taken to be that region of the workpiece subjected to strains >0.2, then this zone thickness is ~40 μm and 85 μm for $\gamma = +10°$ and $-30°$, respectively (Fig. 2). The subsurface deformation increases with decreasing γ and is, thus, controllable. Fig. 3a shows the effect of h_o on subsurface deformation for $\gamma = +20°$. The surface strains estimated by extrapolation are 1.4, 1.7 and 1.5, for $h_o = 50$ μm, 100 μm and 250 μm, respectively, indicating little effect of h_o on surface strain. However, the subsurface deformation increases with h_o. The deformation zone thickness is ~10 μm, 20 μm and 40 μm for $h_o = 50$ μm, 100 μm and 250 μm, respectively. Interestingly, when the data in Fig. 3a are re-plotted against d/h_o, a single exponential curve results (Fig. 3b). Thus, for a fixed γ, the subsurface strain distribution is controlled by a single, non-dimensional parameter – d/h_o. And the thickness of the subsurface deformation zone is $\sim 0.2h_o$ for $\gamma = +20°$ (Fig. 3b). These observations indicate that the subsurface strain is self-similar, scaling with h_o, analogous to wedge indentation.

The large plastic strains on the surface have important implications (like residual stress) for performance of structural components. These strains generally result in refinement of microstructure with attendant Hall-Petch type strengthening [7,8]; they may also reduce ductility of a material making it more prone to cracking and fatigue. The detailed measurements of deformation (including tensor) histories also offer much scope for validation and improvement of machining models.

3.2. Comparison of deformation in chip and surface

Deformation histories of the chip and machined surface were examined. The PIV strain values on the surface are not much